WCCM V
Fifth World Congress on
Computational Mechanics
July 7–12, 2002, Vienna, Austria
Eds.: H.A. Mang, F.G. Rammerstorfer,
J. Eberhardsteiner

Wavelet Based Methods in Elastoplasticity and Damage Analysis

Giovanni Naldi*

Dipartimento di Matematica
Università di Milano, Via Saldini 50, I-20133 Milano, Italy
e-mail: giovanni.naldi@mat.unimi.it

Paolo Venini

Dipartimento di Meccanica Strutturale
Università di Pavia, Via Ferrata 1, I-27100 Pavia, Italy
e–mail: venini@cpmec.unipv.it

Karsten Urban

RWTH Aachen
Inst. f. Geometrie u. Prakt. Mathematik, Templegraben 55, 52056 Aachen, Germany
e–mail: urban@igpm.rwth-aachen.de

Key words: Wavelet Analysis, Multiscale Methods, Plasticity, Adaptivity, Damage Mechanics

Abstract
In this work we review some applications of wavelet bases for the discretization of non linear problems arising in engineering materials. In particular, we will consider a Wavelet-Galerkin method coupling with interpolating bases for the numerical treatement of elastoplasticity problems. Here, we use an elastic predictor/plastic corrector method in terms of a stress correction. This correction has to be done pointwise. We use interpolatory wavelets in the correction step and perform (fast) change of bases to switch between the different representations. We show the basic properties of the new numerical approach by some numerical test both in dynamical case. Moreover,we consider the possibility to state adaptive algorithms for the computation of the plastic wave. A simple one dimensional problem is used, both in hardening and softening case, for numerical test.

1 Introduction

Often the behaviour of the engineering materials is non linear due to the acting forces which bring the material beyond the elastic limit. The classical theory of plasticity is mostly used since it allows a modelling that could be experimentally corroborated. It is well known that a classical problem in the analysis of elastoplastic media is the computation of the mechanical response of a body subjected to some prescribed history of loading/unloading. Commonly, a closed form solutions are not possible then numerical methods must be considered. However, the numerical treatement of elastoplasticity problems is still a challenging and active field of research (see for example, [2, 33, 35, 37]).
Classical methos, such as Finite Differences, Finite Elements, Spectral Elements and others, are proposed for the numerical simulation of these non linear models. More recently, some steps using wavelet bases have been made for the discretization of elastoplaticity problems [9, 24, 32], and A collocation method based on interpolatory wavelet [4], was used in [31] for structural mechanics problems (linear and nonlinear).
We point out that Wavelet transform and wavelet bases were originally conceived as a powerful tool for signal and image processing, but in the last years significant progress has been made for using Wavelet based methods for the numerical solution of various operator equations including elliptic partial differential equations, boundary integral equations and also saddle point problems (see e.g. [3, 6, 13, 15, 26, 36]). Within this framework it is possible, for example, to build suitable preconditioners for a given problem as well as consider new fast and higher order adaptive algorithms by using wavelet bases.
One key ingredient for the analysis here is the use of *semi-orthogonal* and *biorthogonal* wavelet bases within a Galerkin discretization. Moreover, we consider the "classical" elastic predictor/plastic corrector method in terms of a stress correction. This correction has to be done pointwise. In the following we briefly describe a simple one dimensional test model and a suitabl wavelet method for its numerical discretization. We consider the basic properties of the new numerical approach showing some numerical test in dynamical case. In particular we suggest the possibility to state adaptive algorithms for the computation and the prediction of the plastic wave.
Finally, we consider some numerical experiments in the softening case by using a "wavelet detector".

2 A simple one dimensional model

We study, as a test problem, the dynamic response of straight elastoplastic rod. Referring to Figure 1, the space variable is denoted by x, the time variable by t and $u(x,t)$ is the axial displacement of the rod. The physical problem is governed by classical relations expressing equilibrium between applied forces and induced internal stresses, compatibility between displacements and strains and the nonlinear constitutive law that relates stresses to strains. As to equilibrium one may write

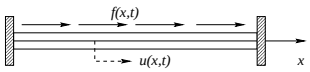

Figure 1: The rod as a simple test problem.

$$(A\sigma)' + f = \rho\ddot{u}, \tag{1}$$

where $A(x)$ and $\rho(x)$ are the cross section and the mass density per unit length, $f(x,t)$ is the axial force and σ is the axial stress. Furthermore, space and time differentiation are indicated by a superposed

prime and dot, respectively. The hypothesis of small displacement gradients will be made under which the compatibility condition may be written as $\varepsilon = u'$, in which $\varepsilon(x,t)$ is the axial strain of the rod. The elastoplastic constitutive law classically needs to be introduced in incremental form since the stress does not only depend on the current strain as it happens in the purely elastic case, but also on the entire past history of it. For clarity sake, we first remark that the purely *linear*–elastic problem is governed by a constitutive law that reads $\sigma = E\varepsilon$, in which E is the Young modulus. Therefore, by eliminating stress and strain in the previous equations, one ends up with a wave equation having the displacement u as unknown, i.e.

$$\big(EAu'\big)' + f = \rho\ddot{u}. \tag{2}$$

2.1 Hardening case

We now introduce the basic incremental relationships defining the elastoplastic behavior of the rod. The main hypothesis, widely used and accepted in the literature, [35], is the additive decomposition of the total strain rate $\dot{\varepsilon}$ into its elastic and plastic contributions, i.e., $\dot{\varepsilon} = \dot{\varepsilon}^e + \dot{\varepsilon}^p$. The stress rate $\dot{\sigma}$ may then be written in terms of any of its above described contributions by introducing the tangent modulus E_t and the plastic one E_p, see Figure 2. These are defined by the following relations

$$\dot{\sigma} = E_t\dot{\varepsilon} = E\dot{\varepsilon}^e = E_p\dot{\varepsilon}^p, \tag{3}$$

where Figure 2 visualizes the introduced quantities. Notice that in Figure 2, σ_{Y_1} is the so called (tension)

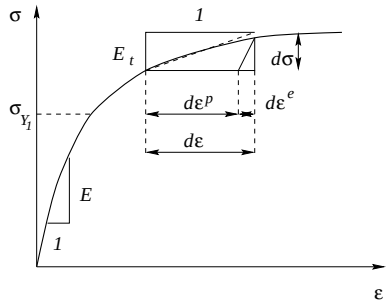

Figure 2: Stress and strain increments.

yielding stress, that is to say the stress above which the material is no longer elastic but undergoes permanent, unreversible deformations. Furthermore, σ_{Y_1} is a variable itself and is to be updated at each time instant according to the so called *hardening rule* that will be discussed next. From a computational point of view, the difficulty is that one does not know in advance whether a stress or strain increment will cause plastic loading or elastic unloading. We assume the rod to be stress–free for $t = 0$ and to behave elastically as long as $(t,x) \in I$ where I is the instantaneous elastic domain defined as

$$I := \{(t,x) \in [0,T] \times [0,1] : -\sigma_{Y_2}(t,x) \leq \sigma(t,x) \leq \sigma_{Y_1}(t,x)\} \tag{4}$$

In (4), σ_{Y_1} and σ_{Y_2} are the yielding stresses in tension and compression, respectively. For $t = 0$ the yielding stresses are known from experimental tests and they evolve with time following some *hardening rule*. The key point is that σ_{Y_1} and σ_{Y_2} depend on each other so that it is convenient to separate the total plastic strain into its tension and compression components. Plastic strains may accumulate if and only if both the current stress state and its update belong to the boundary of the elastic domain. If this is not

the case an elastic phase takes place. Then, in the case of the kinematic hardening rule, we obtain the following problem (for the important topics of the internal variables and of the plasticity functions we refer to the literature cited in the bibliography) where we assume that the ends of the bar are fixed.
Problem 1*For given ρ, E, E_t, E_p, A and f we seek for u, ε and σ such that:*

$$\rho(x)\,\ddot{u}(t,x) - \big(E(x)\,A(x)\,u'(t,x)\big)' = f(t,x), \qquad (t,x) \in I, \tag{E}$$

and

$$\begin{aligned} \rho(x)\,\ddot{u}(t,x) - \big(A(x)\,\sigma(t,x)\big)' &= f(t,x), \quad (t,x) \notin I, \\ u'(t,x) - \varepsilon(t,x) &= 0, \quad (t,x) \notin I, \\ \dot{\sigma}(t,x) - E_t(\sigma(t,x))\,\dot{\varepsilon}(t,x) &= 0, \quad (t,x) \notin I, \end{aligned} \tag{P}$$

Finally, we pose the following initial and boundary conditions

$$u(0,x) = u_0(x), \quad u'(0,x) = u_1(x), \qquad x \in [0,1], \tag{B_1}$$

for some given functions u_0 and u_1, as well as

$$u(t,0) = u(t,1) = 0, \qquad t \in [0,T]. \tag{B_2}$$

In the numerical test we will also consider the case of the softening rule. In this last case, when the elastic limit is reached, the stress–displacement curve has a negative slope as in Figure 3.

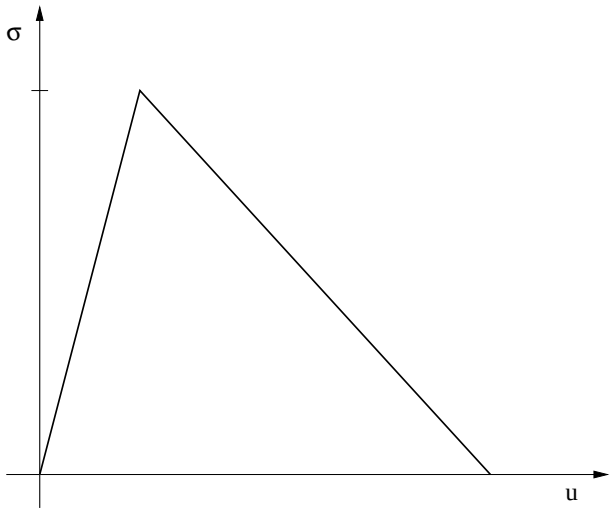

Figure 3: Stress–displacement relation in the case of softening

3 Wavelet analysis

Wavelet transform and wavelet bases are a powerful tool for multiscale data analysis. The goal of such technique is to develop representations of a function at various level of resolution. Typical applications are related to analysis of signals, image compression, edge detection, computational geometry, denoising and so on. The hierarchical structure of wavelets makes them particularly appealing tools for the numerical solution of partial differential equations. In fact wavelet bases provide some good features for solving

differential problems: they constitute unconditional bases for many functional spaces (such as Sobolev spaces), they also provide diagonal preconditioners for elliptic problems. Moreover, due to their good localization and cancellation properties, wavelet bases provide an effective method for data compression when dealing with functions with local singularities. In the last few years different algorithms have been successfully tested on linear and nonlinear partial differential equations, see [13] for a recent review. In this work we will consider the hierarchical structures of the wavelets, and use them for the solution of the initial-boundary value problems arising in elastoplsticity. However, we restrict ourselves to those facts only, that will be used in the sequel and refer e.g. to [6, 13, 19] for textbooks and general surveys on wavelets. A system of compactly supported $L^2(0,1)$–functions $\Psi := \{\psi_\lambda : \lambda \in \mathcal{J}\}$, where $\mathcal{J}$ is an (infinite)set of indices, is called a *wavelet basis* if Ψ spans $L_2(0,1)$ and the following norm equivalence holds

$$\left\| \sum_{\lambda\in\mathcal{J}} d_\lambda \psi_\lambda \right\|_{L_2(0,1)} \sim \left(\sum_{\lambda\in\mathcal{J}} |d_\lambda|^2 \right)^{1/2}, \tag{5}$$

where $A \sim B$ denotes $cA \le B \le CA$ for absolute constants $0 < c \le C$. One can think of $\lambda \in \mathcal{J}$ as a pair

$$\lambda = (j,k), \qquad |\lambda| := j,$$

where $j \in \mathbb{Z}$ denotes the *scale* or *level* of ψ_λ whereas k indicates its location in space (e.g., the center of the support of ψ_λ). Equation (5) implies that Ψ is a *Riesz basis* of $L_2(0,1)$. By Riesz Representation Theorem, (5) implies the existance of a *dual* wavelet basis $\tilde{\Psi} := \{\tilde{\psi}_\lambda : \lambda \in \mathcal{J}\}$, i.e.,

$$(\psi_\lambda, \tilde{\psi}_{\lambda'})_{L_2(0,1)} = \delta_{\lambda,\lambda'}, \qquad \lambda, \lambda' \in \mathcal{J}. \tag{6}$$

The pair Ψ, $\tilde{\Psi}$ is often termed *biorthogonal wavelet system*. The corresponding wavelet spaces which will be used to spatial discretization of **Problem 1** are then given by suitable subsets of Ψ in the following way. For any (finite) subset $\Lambda \subset \mathcal{J}$, we define $\psi_\Lambda := \{\psi_\lambda : \lambda \in \Lambda\}$ and the induced wavelet space by

$$S_\Lambda := \operatorname{span} \Psi_\Lambda.$$

In the following, we consider the spaces $S_j := S_{\mathcal{J}_{[j]}}$, where $\mathcal{J}_{[j]} := \{\lambda \in \mathcal{J} : |\lambda| \le j\}$. These spaces are also often termed as *multiresolution spaces*. It has been proven [13] that under suitable assumptions on the order of approximation and the regularity (direct and inverse estimates) of both Ψ and $\tilde{\Psi}$, (5) indeed holds for a whole range of Sobolev spaces including $L_2(0,1)$. To be more precise, one has

$$\left\| \sum_{\lambda\in\mathcal{J}} d_\lambda \psi_\lambda \right\|_{H^s(0,1)} \sim \left(\sum_{\lambda\in\mathcal{J}} 2^{2s|\lambda|} |d_\lambda|^2 \right)^{1/2}, \qquad s \in (-\tilde{\gamma}, \gamma), \tag{7}$$

where γ, $\tilde{\gamma} > 0$ depend on Ψ, $\tilde{\Psi}$ and $H^s(0,1)$ denotes the usual Sobolev spaces. It turns out that (7) is indeed the key for the strong analytical properties of wavelets for multilevel preconditioning and adaptivity [13]. Usually, the starting point for the construction of wavelet bases is a second system of functions $\Phi_j := \{\varphi_{j,k} : k \in \mathcal{I}_j\}$ (where again $\mathcal{I}_j$ is a suitable set of indices), that are *refinable*, i.e.,

$$\varphi_{j,k} = \sum_{l\in\mathcal{I}_{j+1}} a^j_{k,l}\, \varphi_{j+1,l}, \qquad k \in \mathcal{I}_j, \tag{8}$$

for suitable refinement coefficients $a^j_{k,l} \in \mathbb{R}$. This implies that the generated spaces $S_j = \operatorname{span} \Phi_j$ are *nested*: $S_j \subset S_{j+1}$. A similar construction is done for the dual system, which we will always indicate

by a superposed '˜'. The systems Φ_j, $\tilde{\Phi}_j$ are often referred to as *primal* and *dual scaling systems*. The biorthogonal wavelet spaces W_j, $\tilde{W}_j$ are defined by

$$W_j := S_{j+1} \ominus S_j, \;\; \tilde{W}_j := \tilde{S}_{j+1} \ominus \tilde{S}_j, \qquad S_j \perp \tilde{W}_j, \;\; \tilde{S}_j \perp W_j,$$

where orthogonality is to be understood w.r.t. the $L_2(0,1)$–inner product. Finally, the wavelets $\psi_\lambda = \psi_{j,k}$, $\tilde{\psi}_\lambda = \tilde{\psi}_{j,k}$ are constructed as a suitable basis for W_j, $\tilde{W}_j$, respectively, i.e.,

$$W_j = \operatorname{span} \Psi_j, \qquad \Psi_j := \{\psi_{j,k} : \, k \in \mathcal{J}_j\}, \quad \mathcal{J}_j := \mathcal{I}_{j+1} \setminus \mathcal{I}_j,$$

(similar for $\tilde{W}_j$) and $(\psi_{j,k}, \tilde{\psi}_{j',k'})_{L_2(0,1)} = \delta_{j,j'}\delta_{k,k'}$, see also (6). Roughly speaking the space W_j contains the "details" needed going from an approximation at level (scale) j to an approximation at level $j+1$. The maybe easiest situation occurs if one considers $L_2(\mathbb{R})$ instead of $L_2(0,1)$. There, a wavelet basis Ψ can be constructed from a single *mother wavelet* ψ by taking integer translations of dyadic scaled versions of ψ [19], i.e.,

$$\psi_{j,k}(x) := 2^{j/2}\psi(2^j x - k), \qquad j,k \in \mathbb{Z}. \tag{9}$$

On $[0,1]$, one takes as many functions of the form (9) as possible (namely those that are supported strictly inside $[0,1]$) and perform suitable adaptations near the boundary points in order to preserve biorthogonality, regularity and approximation order, see e.g. [1, 6, 14, 23], where this list is far from being complete. A very simple, but not smooth, example of scaling function, is given by $\phi(x) = \chi_{[0,1]}(x)$, the characteristic function of the unit interval, the subspace S_0 is composed of piecewise constant functions. The corresponding wavelet, named *Haar wavelet*, is defined by $\psi(x) = \phi(2x) - \phi(2x-1)$. The lack in information between two successive levels can be coded with functions $\psi_{j,k}$ in the subspace W_j. One of the most attractive features of wavelets is that they give completely local information on the functions analyzed. In order to consider this last property we could consider a suitable microlocal space $C^s_{x_0}$, introduced by Jaffard [25]. Nowadays, many families of wavelet constructions are available. We chose here biorthogonal spline wavelets, [7]. In this case, the primal scaling system is build by cardinal B–splines ${}_dN$ of order $d \in \mathbb{N}$. Then, dual scaling systems generated by some functions ${}_{d,\tilde{d}}\tilde{N}$ for $d + \tilde{d}$ even can be found in the literature, [7]. The regularity and approximation order of ${}_{d,\tilde{d}}\tilde{N}$ is related to $\tilde{d}$ and can be chosen arbitrarily high (with the dispense of increasing size of their support, however). The adaptation of this construction from $L_2(\mathbb{R})$ to $L_2(0,1)$ has been studied in many papers [1, 14, 23] and we choose the bases from [14] here. Another possibility is considered here in order to have hierarchical wavelet bases with some "easy" recipe for the treatment of boundary conditions. In some sense we relax the orthogonality conditions of wavelet basese but retaining the good properties of wavelets system. In the first one case we consider a finite-element like basis but with orthogonal hierarchical arrangement. We propose to keep on using the calssical tent functions of linear finite element at an initial scale and try to capture new details by introducing semi-orthogonal wavelets [9, 13, 22] centered in between two tent functions. We lost the orthogonality between the scaling/wavelet functions and their translate version but we preserve the orthogonality between two different scale. In Figure 4 the shape of our scaling and wavelet functions are shown. Boundary conditions may be imposed substituting at the boundaries the ordinary wavelet $\psi(x)$ by $\psi_D(x)$ and $\psi_N(x)$ (see Figure 4), in the case of Dirichlet or Neumann conditions, respectively.

4 Numerical approximation and numerical results

Here the approach is in two steps: first an elastic trial state is computed, then if this lies outside the elastic region it is porjected onto the yeld surface to find the new stress state. Let us start by a brief description

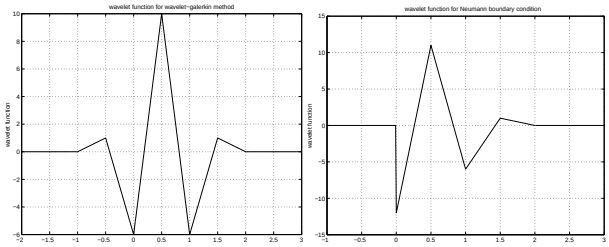

Figure 4: Scaling and wavelet functions for 1D elastoplasticity problem and Wavelet function for boundary condition.

of this elastic predictor–plastic corrector strategy. There exist several cases to be handled numerically, for clarity sake we hereafter focus on one of them, i.e. the case of plastic loading or elastic unloading in tension. Let the converged stress $\sigma(t,x)$ is on the boundary of the instantaneous elastic domain, given is also $u(t,x)$ for some time t. Then, for a given $\Delta t > 0$, we compute the *elastic predictor* $u^*(t+\Delta t,x)$ by solving the problem (E) (we will omit explicity refering to initial/boundary conditions) all the time). Then, by using the second equation in (P) we compute the elastic strain ε^* and then we obtain the elastic trial stress σ^*. If $\sigma^* < \sigma_{Y_1}$ then an elastic unloading has taken place and therefore $\sigma(t+\Delta t,x) = \sigma^*$ and no correction is required. If conversely $\sigma^* > \sigma_{Y_1}$, a strain–driven modified Newton–Raphson correction scheme is used and illustrated in Figure 5. We only point out that, in the plastic case, the

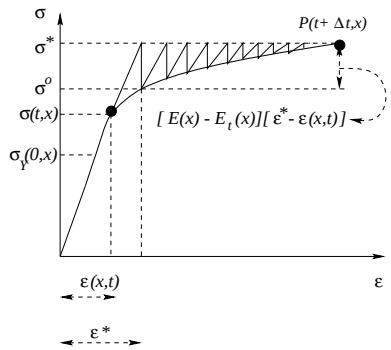

Figure 5: The prediction–correction procedure.

quantity $A(x)[\sigma^* - \sigma^o](t,x)$ becomes a virtual, un–equilibrated force that is brought to the right–hand side of Equation (E) so as to allow the computation of a further update for the displacement and for the strain ε. The procedure ends when the actual stress–strain curve joins the plateau σ^* where the solution in terms of stress, strain and displacement is attained (point $P(t+\Delta t,x)$ in Figure 5). Notice that σ^* is not only the stress $\sigma(t+\Delta t,x)$ but also the new value of the yielding stress σ_{Y_1} to be used for the subsequent stress computation. When linear isotropic hardening is adopted,the whole stress correction procedure is governed by eight alternative cases, for details see [32]. In each time t_n we will approximate the solution of equilibrium equation by means of a wavelet expansion of the type

$$u(t_n,x) \sim \sum_{\lambda\in\mathcal{I}} u_\lambda(t)\Psi_\lambda(x) := u_n(x),$$

where λ denotes the indices (j,k), $\mathcal{I}$ a set of indices, Ψ a set of wavelet (scaling or wavelet functions) and $u_\lambda(t)$ are suitable coefficients. Then, the Galerkin approximation of (E) reads

$$\sum_{\lambda\in\mathcal{I}} \left\{ \ddot{u}_\lambda(t) < \rho\psi_\lambda, \psi_m u > + u_\lambda(t) < EA\psi'_\lambda, \psi'_\mu > \right\} = < f, \psi_\mu >, \qquad \mu \in \mathcal{I},$$

Hence, we obtain the system

$$M\,\ddot{X}(t) + K\,X(t) = F(t), \tag{10}$$

with the following parameters

$$\begin{aligned} M \quad &= M_n^\rho \quad := (< \rho\psi_\lambda, \psi_\mu >)_{\lambda,\mu\in\mathcal{I}}\,, \\ K \quad &= K_n^{EA} \quad := \left(< EA\psi'_\lambda, \psi'_\mu >\right)_{\lambda,\mu\in\mathcal{I}}\,, \\ X(t) \quad &= U_n(t) \quad := (u_\lambda(t))_{\lambda\in\mathcal{I}}\,, \\ F(t) \quad &= F_n(t) \quad := (< f(t,\cdot), \psi_\mu >)_{\mu\in\mathcal{I}}\,. \end{aligned}$$

In (10) the mass matrix M and the stiffness matrix K are symmetric, K is positive (semi-)definite and M is positive definite. By using wavelet bases (also semi-orthogonal or biorthogonal) the matrices M and K have a typical "finger block structure". Moreover it is possible to build diagonal preconditioners which give an $O(1)$ uniform condition number [6, 13, 26]. Computing integrals of (products of derivatives of) wavelets as those in the above matrices is a numerical topic for which the reader is referred to [36] where computing integrals of wavelets is shown to be equivalent to solving a proper eigenvalue problem (as first proposed by Dahmen and Micchelli). Time integration of the system (10) on the time interval $\Delta t = t_{n+1} - t_n$ is carried over using a second order unconditionally stable Newmark scheme having as unknowns the coefficients $X(t)$. It is interesting to note that these coefficients do not represent nodal values of the field being approximated as would happen with conventional finite elements. Then it seems that, in a certain sense, the Galerkin method for the discretization in space contradicts the elastic–predictor plastic–corrector strategy. The latter involves *point values* of the basis functions whereas the Galerkin discretization only uses *integrals* over (products of derivatives of) these functions. The reasons for using a Galerkin approach have been detailed above. However, the pointwise correction is physically adequate. In the case of semi-orthogonal wavelet we have a nodal basis as in linear finite element method and we can perform the correction without any further difficulties. For biorthogonal basis we performed a mixture of the two methods as described below. For the discretization in space we use a Galerkin method with biorthogonal spline wavelets. When it comes to the stress correction, we perform a fast change of basis to an interpolatory wavelet basis where the correction can easily be performed. The resulting unequilibrated force serves as a right–hand side in an elliptic problem. Hence, it is rather easy to perform an L_2–projection of this function in order to determine the entries of the right hand side. This approach allows us to combine two advantages, namely the use of mathematically founded Wavelet–Galerkin methods with biorthogonal wavelets and an efficient stress correction using interpolatory wavelets [32].

5 Numerical results

In this section we summarize some of the numerical experiments that have been performed. In the first test we consider a uniform bar extending over the domain $\Omega = [0,1]$, $A(x) = 100$, $\sigma_{Y_1} = -\sigma_{Y_2} = 1600$, $E = 2100000$, $\rho(x) \equiv 7.85$, $E_t = 200000$, $dt = 0.01$. The applied load is given as

$$f(x,t) = \begin{cases} g(t) & 0 \le x \le 1/2, \\ 0 & 1/2 < x \le 1 \end{cases} \tag{11}$$

where $g(t)$ is a time dependent signal. We use the semi-orthogonal basis with initial scale $j_0 = 3$, amounting to eight conventional finite elements as far as the tent functions are concerned. Wavelet analysis is carried on up to the next level. The global displacement response with respect to space and time is shown in Figure 6 with the projection of the response into the subspace V_3 (coarse space), W_3, W_4 (that is to say scaling coefficients $c_{3,k}$, and wavelets coefficients $d_{3,k}$, $d_{4,k}$). Due to to the identity $V_5 = V_3 \oplus W_3 \oplus W_4$, the computed global response is exactly the same one would obtain with an ordinary linear finite element analysis, moreover it has a regular behavior. However, One may see that an irregular behavior is clearly captured for $x = 0$ and $x = 1/2$, by the details in wavelet subspaces W_3 and W_4. The load given by

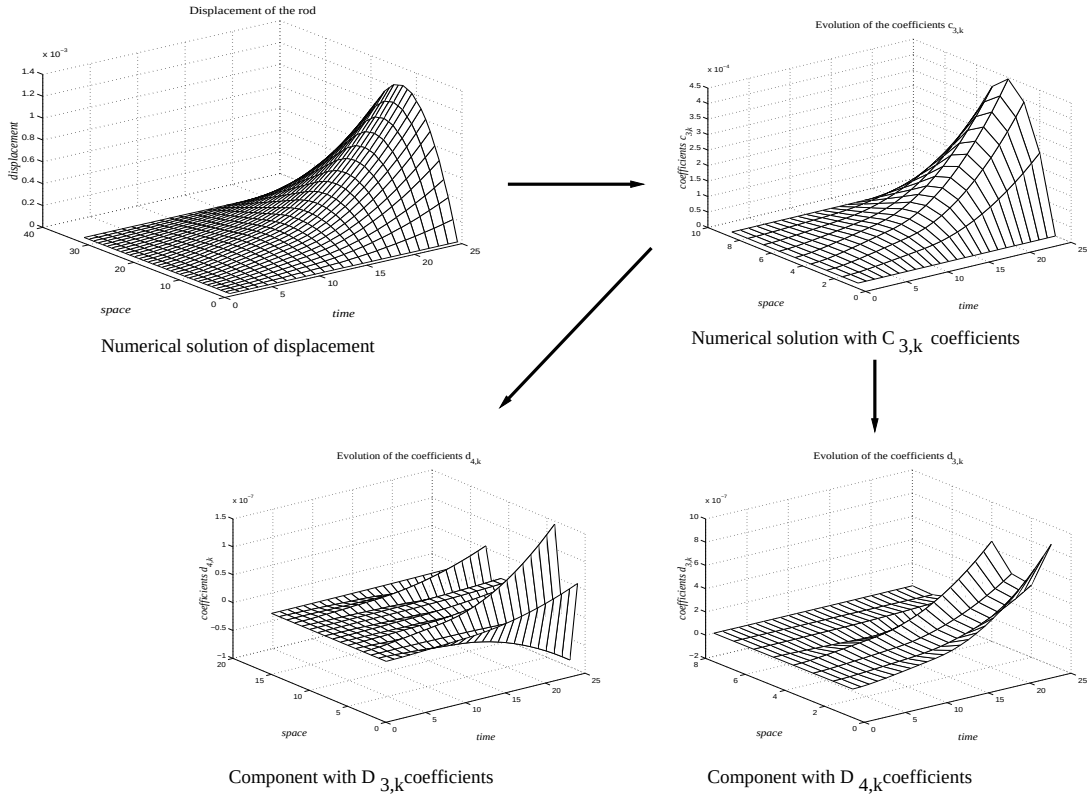

Figure 6: Space–time evolution of the displacemnts and multiresolution decomposition.

equation (11) is discontinuous exactly for $x = 0$ and $x = 1/2$ and all t so that the elastic response of the system has a discontinuous second derivative with respect to the space variable. This discontinuity is then responsible for the jumps one may observe for coefficients $d_{3,k}$ in Figure 6. In other words classic finite element schemes need suitable indicators to detect irregular behaviors and to drive the construction of an adaptive mesh–refinement scheme. The nice feature of the proposed approach is then the possibility of projecting the response into the spaces V_3, W_3 and W_4, gaining this way some insight that is not observable from the global response and to detect singularity.

The spreading of plasticity in the structure may finally be captured by looking at the coefficients $d_{4,k}$ and checked in Figure 7. The latter figure shows a scalar function depending on space and time that takes value one for all the pairs (x, t) for which plastic strains are progressing and zero otherwise. One may see that plasticity starts from the section $x = 0$ at a certain time and progresses toward the midspan. Later on, a second plastic wave originates from the section $x = 1$ and propagates back toward the center of the rod, leaving only a small region in the elastic regime. The two waves are clearly captured by the

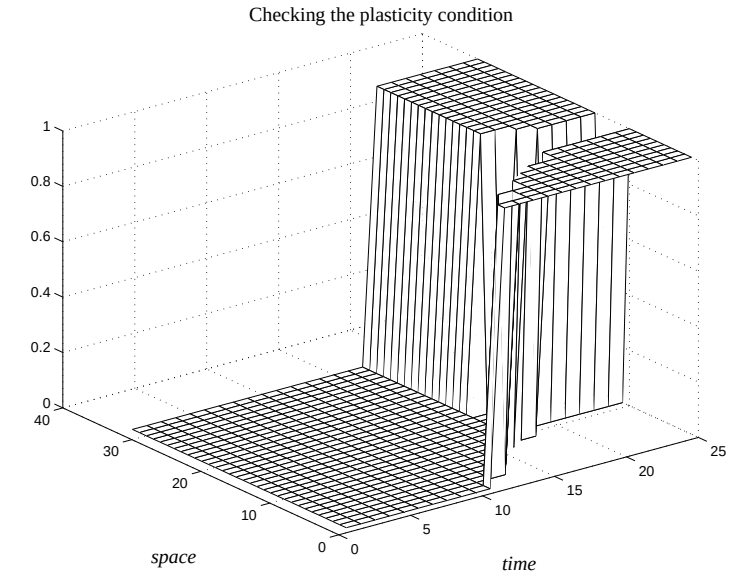

Figure 7: Checking the yielding condition in space and time

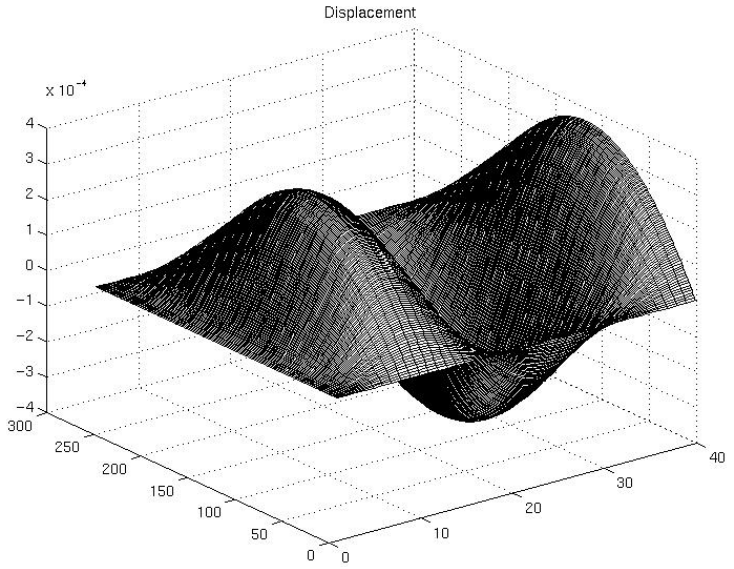

Figure 8: Displacemnet computed by using biorthogonal basis and with a periodic load.

evolution of the $d_{4,k}$ that present two spikes evolving in time. The amplitudes of the spikes are different since such are those of the two plastic waves travelling in the rod.

In the second test we consider a periodic force $f(t,x) := \chi_{[0,0.7]}(x)\, a\, \sin(\omega t),\ \ a = 8 \cdot 10^5,\ \omega = \frac{20}{3}\pi$ and biorthogonal B-spline wavelet. The numerical solution for the displacement is shown in Figure 8, while the characteristic stress/strain curve at the two point $x = 0$ and $x = 0.98$ are displayed in Figure 9. In Figure 10 we have plotted the resulting plastic indicators as describe in the first test. By using different B-spline scaling it is possible to state high order methods for elastoplasticity problems and again wavelet coefficients can point out the plastic regions and detect singularity. This is a first step for a next adaptive numerical scheme [36].

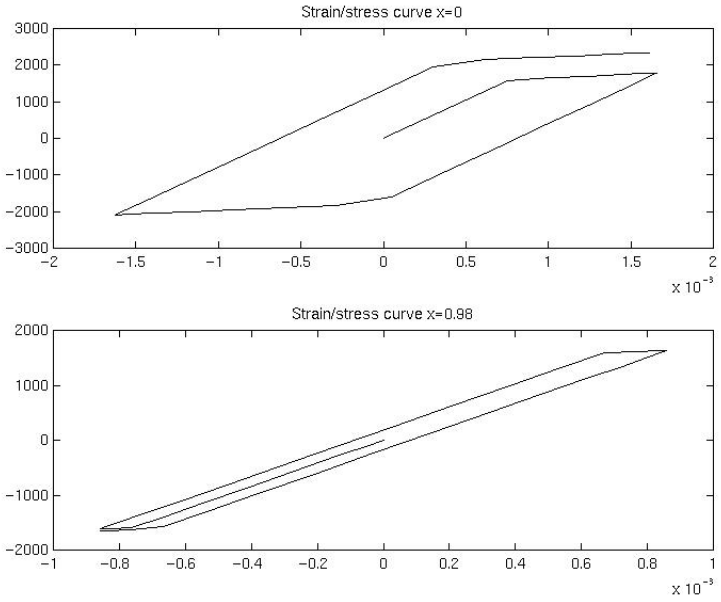

Figure 9: stress/strain curve at two different points.

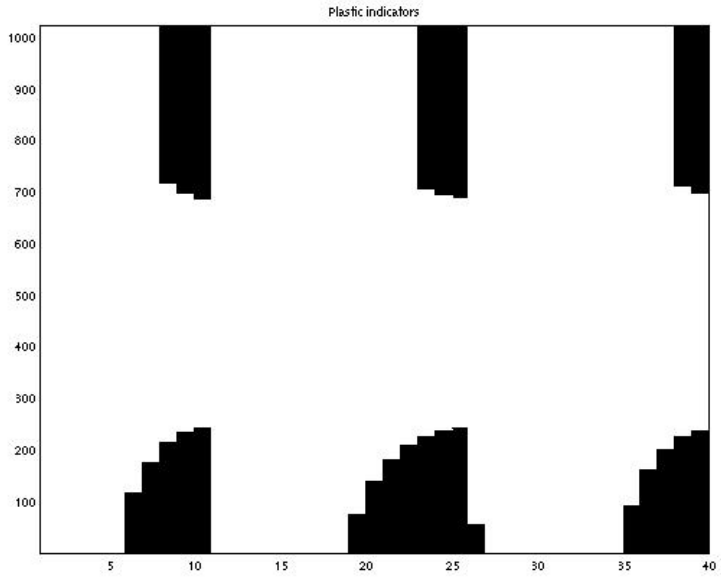

Figure 10: Plastic flags, the $x-$axis corresponds to the time steps and the $y-$axis to the $i/1024$ points in space.